Physics – Uspekhi **43** (5) 493 – 508 (2000)

REVIEWS OF TOPICAL PROBLEMS PACS numbers: 61.25.Mv, **61.43. – j, 62.50. + p**, **66.20. + d**, 91.35.Ed

Universal viscosity growth in metallic melts at megabar pressures: the vitreous state of the Earth's inner core

V V Brazhkin, A G Lyapin

DOI: 10.1070/PU2000v043n05ABEH000682

Contents

Abstract. Experimental data on and theoretical models for the viscosity of various types of liquids and melts under pressure are reviewed. Experimentally, the least studied melts are those of metals, whose viscosity is considered to be virtually constant along the melting curve. The authors' new approach to the viscosity of melts involves the measurement of the grain size in solidified samples. Measurements on liquid metals at pressures up to 10 GPa using this method show, contrary to the empirical approach, that the melt viscosity grows considerably along the melting curves. Based on the experimental data and on the critical analysis of current theories, a hypothesis of a universal viscosity behavior is introduced for liquids under pressure. Extrapolating the liquid iron results to the pressures and temperatures at the Earth's core reveals that the Earth's outer core is a very viscous melt with viscosity values ranging from 10^2 Pa s to 10^{11} Pa s depending on the depth. The Earth's inner core is presumably an ultraviscous ($> 10^{11}$ Pa s) glass-like liquid — in disagreement with the current idea of a crystalline inner core. The notion of the highly viscous interior of celestial bodies sheds light on many mysteries of planetary geophysics and astronomy. From the analysis of the pressure variation of the melting and glass-transition temperatures, an entirely new concept of a stable metallic vitreous state arises, calling for further experimental and theoretical study.

V V Brazhkin, A G Lyapin Institute for High Pressure Physics,
Russian Academy of Sciences
142190 Troitsk, Moscow Region, Russian Federation
Tel. (7-095) 334-0011. Fax (7-095) 334-0012
E-mail: brazhkin@ns.hppi.troitsk.ru

Received 10 November 1999
Uspekhi Fizicheskikh Nauk **170** (5) 535 – 551 (2000)
Translated by E Yankovsky; edited by M V Magnitskaya

1. Introduction

The properties of melts (in contrast to those of solids) have been studied very little. This is especially true of the atomic kinetic properties such as the viscosity and diffusion coefficients. The thermodynamic characteristics of melts of substances (the equation of state, primarily) have been studied somewhat more thoroughly. Measurements have been done in shock-wave experiments up to pressures of roughly 10 Mbar (= 1000 GPa) [1 – 3]. Here there exist fairly well developed theoretical concepts that provide an adequate description of the equation of state up to astronomical pressures of roughly 10^{10} Mbar and higher [4]. The electron transport properties of metallic melts (the electrical conductivity, primarily) have also been studied in experiments in the megabar pressure range, and their behavior is described fairly well theoretically. At the same time, the atomic transport properties of melts under pressure have been studied only for a small number of liquids (mostly non-metallic) and at pressures of about 10 kbar = 1 GPa (in rare cases up to 30 – 80 kbar). The theoretical basis for describing the behavior of atomic transport coefficients in melts under pressure has yet to be developed. The occasional computer calculations of atomic diffusion under pressure from first principles do not yet provide reliable results.

It is difficult to overstate the importance of gaining information about the atomic transport properties of melts under high pressures, since most of the interiors of planets and other celestial bodies are in a liquid state under high static compression. The viscosity and diffusion coefficients of the corresponding melts determine the heat and mass transfer inside celestial bodies, the crystallization kinetics in the event of cooling, the emergence and support of a magnetic field, the natural oscillations of planets, and the tidal forces establishing the dynamics of the rotation of planets and their satellites. According to modern ideas, the outer part of the Earth's core

consists of an iron melt with an admixture of lighter atoms at pressures of $P \sim 1.35-3.3$ Mbar and temperatures of $T \sim 4000-7000$ K [5–10]. The cores of Earth-like planets are probably constituted of iron melts with different admixtures [11]. It is believed that the main fraction of matter in giant planets is hydrogen and helium in a liquid (possibly metallic) state at pressures of tens of megabars and temperatures of several tens of thousands of kelvins [11]. It is also assumed that such objects as white dwarfs are in a partially melted state of an electron–ion plasma at $P \sim 10^{10}$ Mbar and $T \sim 10^7$ K [4].

The pressure gap of 3 to 12 orders of magnitude between the region studied in experiments and the state of metallic melts in celestial bodies presents considerable difficulties for description of the behavior of highly compressed melts and often makes it impossible to choose between one planetary model or another. The problem is not only that the description of the corresponding physical characteristics is purely quantitative but also that the most important fundamental problems remain unresolved. For instance, it is known that many dielectric melts are transformed under pressure into the glassy state. The vitrification process usually takes place in the metastable (supercooled or 'overcompressed') region with respect to the melting curve $T_m(P)$. It is unclear whether vitrification of metallic liquids under high pressures is possible. The question of the mutual position of the melting and glass-transition lines for melts under megabar pressures is also of considerable interest.

The present review is an attempt to systematize the results of experimental studies of, and the theoretical approaches to, the description of the viscosity of the liquid state under high pressure (Section 2). The original studies of the viscosity of iron and other melts of metals along the melting curve (Section 3) have made it possible to choose the correct empirical models and make an assumption concerning the universal nature of viscosity variations along the melting curve for melts of various classes of substances (Section 4). The results of a critical review of the literature, the experimental studies, and a detailed analysis of the existing ideas have made it possible to develop approaches to a theoretical description of the behavior of melts under megabar pressures (Sections 5, 6, and 8) and to formulate new concepts concerning the inner structure of the Earth and other planets (Section 7).

2. Viscosity of the liquid state of matter under high pressure

2.1 Experimental studies

Experimental studies of the viscosity of liquids under high pressure are usually conducted at moderate temperatures (100–400 K) using methods such as the falling cylinder or ball method [12–15], the vibrating crystal or string method [15, 16], and the method in which the drop of pressure in capillaries is measured [17, 18]. During recent years several new methods have been developed for measuring the viscosity of a liquid including the viscosity of highly viscous states, in diamond-anvil cells [19]. When a substance is under pressure, its viscosity η can be directly estimated from the value of the self-diffusion coefficient D: the values of D and η in melts are linked through relations of the Stokes – Einstein type,

$$\eta \sim \frac{kT}{DL}\,, \qquad (1)$$

where k is Boltzmann's constant, T is the temperature, and L is a slowly varying parameter with dimension of length. Experimental studies of diffusion in liquid metals under pressure were conducted using a method in which the concentration profile of a radioactive isotope is measured [20]. Formula (1) is valid for a liquid state in a fairly general case [21–23] within a broad range of viscosities, from 10^{-4}–10^{-2} Pa s (the viscosity of liquid metals and rare-gas liquids) to 10^3-10^5 Pa s (the viscosity of certain organic liquids). Note, however, that recently conducted studies [24–27] have revealed the presence of systematic deviations from (1) for large viscosity values, $\eta > 10^3$ Pa s. The violation of the Stokes – Einstein law is due to the heterogeneous nature of diffusion in viscous liquids on nanoscales and the resulting ambiguity in averaging the diffusion coefficients [24, 25]. When the viscosity is high, $D \sim \eta^{-\alpha}$, where α varies in different cases from 0.28 to 0.75 [26, 27].

The melts that have been investigated can be tentatively divided into three groups: (i) melts of metals; (ii) molecular liquids, including organic and inorganic (e.g. H_2O, CCl_4, and CS_2) liquids; (iii) and rare-gas liquids. The viscosity of ionic and covalent melts of inorganic substances under pressure have been studied to a considerably lesser extent.

Reliable viscosity data for metals have only been obtained for Hg at pressures up to 12 kbar [28]. Self-diffusion coefficients of K, Rb, and Na at pressures up to 3–4 kbar have also been studied [20, 29]. The increase in the viscosity and the decrease in the self-diffusion coefficients of metallic melts under compression were found to be insignificant and amounted to several tens of percents (under pressures of about 10 kbar). Very few attempts have been made to study the viscosity of metallic melts under higher pressures. LeBlanc and Secco [30] studied the viscosity of the $Fe_{73}S_{27}$ melt under 20–50 kbar and observed an increase in the viscosity in this pressure interval of several tens of percents. Earlier one of the authors of the present review developed a method for estimating the viscosity and surface tension of melts using the experimental data on supercooling of liquids and the grain size in the crystallized phase (for more details see Section 3) [31–36]. It was found that the viscosity of the melts under investigation increased by two to three orders of magnitude as the pressure was increased isothermally to 80 kbar.

The viscosity of organic liquids increases rapidly and nonlinearly (usually in an exponential manner) with pressure — by one to three orders of magnitudes at pressures of about 10 kbar [12]. At higher pressures, the increase in the viscosity of organic liquids becomes more rapid — by 2 to 7 orders of magnitude at 30 kbar [13] and by 5 to 14 orders of magnitude at 60–80 kbar [15, 17, 19]. Here the value of the viscosity of some of the liquids investigated approaches that characteristic of glass, $10^{12}-10^{14}$ Pa s, provided that crystallization is avoided at the lower pressures. As the glass-transition pressure is approached, the increase in viscosity is faster than that provided by an exponential law (Fig. 1) [15, 17, 19, 37]. Actually, critical behavior is observed as the glass-transition line $T_g(P)$ is approached, in the same way as it is observed in a supercooled liquid. For most of the molecular melts studied under pressure, critical behavior begins at a viscosity in the 10^2-10^6 Pa s range (see Fig. 1) [15, 17, 19]. Note that by their behavior near the glass-transition line liquids can be categorized as 'strong' or 'fragile' [38]. For strong liquids the Arrhenius exponential temperature dependence is observed up to the vitrification region, while for fragile liquids the exponential behavior is replaced by a more

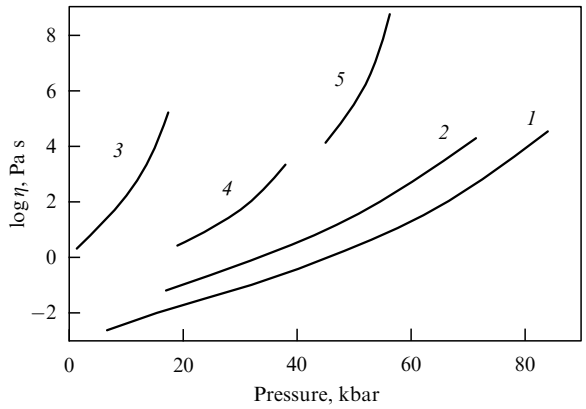

Figure 1. Experimental curves depicting the pressure dependence of viscosity for several organic liquids and taken from Refs [15, 17, 19]: 1, methanol; 2, mixture of methanol and ethanol (4:1); 3, toluene; 4, butyl chloride; and 5, ethyl ether. As the pressure grows, the increase in viscosity is faster than that provided by the exponential law.

rapid one at low viscosities, $10^{-1}-10^{6}$ Pa s, and in Arrhenius coordinates the dependence of viscosity is highly non-linear [35]. The majority of organic melts that have been studied under pressure belong to the fragile class. Moreover, it is known that for many liquids the dependence of the viscosity characteristic of strong liquids becomes substantially non-linear under pressure in Arrhenius coordinates and that the behavior of the liquid's viscosity becomes that of a fragile liquid [38].

Rare-gas liquids occupy an intermediate position between organic liquids and metals: their viscosity increases non-linearly by a factor of approximately 10 at pressure of roughly 10 kbar [14, 16]. Attempts have also been made to study the behavior of viscosity under pressure for several melts of ion-covalent crystals such as silicates [39–42] and for sulfur melt [43].

Note that besides studies at static pressures there have been attempts to study the behavior of viscosity using shock-wave compression. The shock-wave compression was used by Mineev and Savinov [44] to study the viscosity of several melts and also by Mineev and Zaidel' [45], Mineev and Savinov [46], and Al'tshuler et al. [47] to study the viscosity of liquid mercury and water under pressures of hundreds of kilobars, but the interpretation of the results was slightly ambiguous [48]. Nevertheless, there is experimental evidence for the possibility that the viscosity of melts increases by several orders of magnitude, e.g. for liquid water at pressures of roughly 100 kbar [46, 47].

Summing up the experimental data for different types of substance, we conclude that for all melts the viscosity increases with pressure non-linearly. The rate of viscosity growth with pressure is different for different types of liquid: roughly 10% at 10 kbar for metals; roughly 10 times at 10 kbar for rare-gas liquids; roughly 10^{1} to 10^{6} times at 10 kbar for organic liquids; and 10^{5} to 10^{14} times for organic liquids at 50–80 kbar. Unfortunately, most measurements have been done in isothermal conditions, and there have been only a few attempts to study experimentally the behavior of viscosity under pressure at different temperatures.

Liquid metals have smaller compressibility than molecular melts and rare-gas liquids [49, 50]. As a result, the already moderate range of pressures in which studies of the viscosity and diffusion coefficients have been conducted corresponds to a very small value for the compression of metallic melts (several percents). The correspondingly small variation of the viscosity of melts and the lack of systematic measurements of the temperature dependence of viscosity under pressure makes it extremely difficult, on the one hand, to extrapolate the experimental curves into the megabar pressure range and, on the other, to compare the experimental data for liquid metals with the different theoretical models.

Note that diffusion in crystals under pressure has been studied much more thoroughly and in a broader pressure range than the viscosity of melts. In contrast to liquids, most crystals (including metallic crystals) exhibit fairly universal behavior: an exponential slow-down in the diffusion coefficients (with increasing pressure) by one to four orders of magnitude at pressures in the 20–50 kbar range [51, 52].

2.2 Empirical models

The different classes of substances under investigation are associated with different theoretical approaches for describing the viscosity of liquids under pressure. Calculations of the viscosity and the self-diffusion coefficients from first principles are difficult and were carried out only for the simplest model systems such as a gas of hard spheres of a moderate density [53–55]. Formally, the self-diffusion coefficient is related to the autocorrelation function of velocity through the following formula [56, 57]:

$$D=\frac{1}{3}\int_0^\infty \overline{v(0)v(t)}\,\mathrm{d}t\,.$$

Attempts to calculate such autocorrelation functions were made primarily for particles with a homogeneous potential function of the interaction [56] and, in particular, for hard spheres [53–55].

Various empirical models are used to describe real melts of substances belonging to different classes. In most melts the viscosity grows with pressure but decreases as the temperature increases. Obviously, in the P, T plane there must be lines with a positive slope corresponding to the condition for the constancy of viscosity. There are some 'physically preferred' lines with a positive slope in the P, T plane: the melting curve, isochores, adiabates, etc. There is no sufficient reason to believe that some of these lines correspond to a constant viscosity. Nevertheless, one is tempted to interpret the experimental data using simple empirical models.

Theoretically speaking, there are two empirical approaches here: (i) the viscosity is constant along the melting curve [23], and (ii) the viscosity is constant along isochores [12, 13]. Note that these approaches produce essentially different predictions concerning viscosity behavior, since the isochore slope in the P, T plane is usually 2 to 20 times larger than the slope of the corresponding melting curves [49, 58].

The Arrhenius activation model,

$$\eta=\eta_0\exp\left(\frac{E_{\mathrm{act}\,0}+PV_{\mathrm{act}}}{kT}\right), \qquad (2)$$

is widely used to describe the viscosity behavior of all types of melts [23]. It is usually assumed that the activation energy E_{act} is a linear function of pressure, $E_{\mathrm{act}}=E_{\mathrm{act}\,0}+PV_{\mathrm{act}}$, where V_{act} is the corresponding activation volume. There are good reasons to use the activation model to describe the behavior of the viscosity of liquids. As noted earlier, viscosity is related to

diffusion, which is mainly determined by activation processes, at least in solids. Moreover, in the solid state (crystals and amorphous solids) the diffusion processes are adequately described by the activation model. Here the activation volume changes little with pressure and is, for different substances, $(0.3-1.5)V_{at}$ [37, 52], where V_{at} is the atomic volume, and under high pressure (>20 kbar), $(0.3-0.4)V_{at}$ [51].

Several models for describing the viscosity of metallic melts have been proposed. According to the approach developed by Rice and Nachtrieb [59] and Poirier [23], the viscosity of liquid metals does not vary along the melting curve, with the result that the activation model yields

$$V_{act} = E_{act}\,\frac{d\ln T_m}{dP}\,. \tag{3}$$

Here the viscosity depends solely on the reduced temperature T/T_m. This means that all the processes related to viscosity and diffusion (the kinetics of phase transitions, crystallization of the melt, etc.) are also determined by T/T_m [37]. According to the elastic energy model and the theory of activated states [37, 52],

$$V_{act} = C\,\frac{E_{act}}{B}\,, \tag{4}$$

where B is the bulk modulus, and C is a constant that is approximately four. It can be shown that when the Lindemann criterion for melting is met [60], the expressions (3) and (4) are close. Indeed, according to Lindemann law, the melting point is given by the expression

$$T_m \sim V^{2/3}\omega^2\,, \tag{5}$$

where V is the corresponding specific volume, and ω is the Debye frequency. Combining (3) and (5), we get

$$V_{act} \sim \frac{E_{act}}{B} + c\,\frac{\partial\ln\omega}{\partial P}\,,$$

which for weak pressure dependence of $\ln\omega(P)$ agrees with equation (4). Andrade's model [61], according to which the viscosity increases slightly along the melting curve, yields similar results:

$$\eta \sim T_m^{1/2}\rho^{2/3}\,, \tag{6}$$

where ρ is the melt's density. All these models, (3), (4), and (6), correspond to an extremely small effective volume in the activation law (2), amounting to several percent. Moreover, according to these models, the activation volume must decrease under pressure. Experimental data do indeed correspond to small activation volumes of roughly $0.05V_{at}$ [28], although the value obtained for the Na melt was $V_{act} = 0.17V_{at}$ [20].

Note that a certain agreement between the estimates of viscosity of liquid mercury made on basis of models (3), (4), and (6) and the experimental data in the initial range of pressures (where the pressure dependence of viscosity is almost linear), obviously, does not mean that these models can be automatically extended to high pressures. We also note that the presence of a weak pressure dependence of the viscosity along the melting curve has been proved with theoretical rigor only for systems with a homogeneous potential function for interparticle interaction [56].

Explaining the anomalously rapid growth of the viscosity of organic liquids under pressure requires other approaches. The activation law (2) provides a fairly good description of the experimental data for molecular melts under pressure, but only when V_{act} increases from $0.05V_{mol}$ to $0.3V_{mol}$ (Fig. 2), where V_{mol} is the volume per molecule [37]. To describe an increase of viscosity under pressure that is faster than that provided by an exponential law, Souders [62], Sanditov and Bartenev [63], and Doolittle [64] introduced the following empirical approximations.

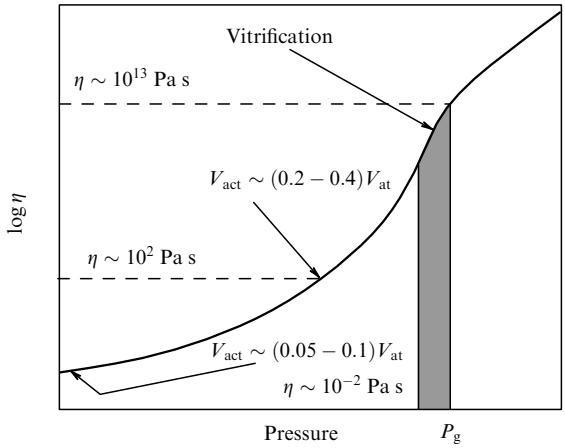

Figure 2. Generalized schematic pressure dependence of the viscosity of melts illustrating the increase in the effective activation volume as the vitrification point is approached. After vitrification is completed (i.e. after the glass transition is passed), the activation volume decreases to the level characteristic of solids.

According to Souders [62],

$$\eta = A_1\exp\left[\exp(A_2\rho - A_3)\right], \tag{7}$$

where A_1, A_2, and A_3 are constants and ρ is the liquid's density, i.e. the viscosity does not vary along an isochore. A slight variation of viscosity along isochores was noted by Bridgman [12, 13]. It would appear, at first glance, that in many respects viscosity is determined by the average distance between molecules, i.e. the density of the melt. However, no rigorous theoretical proof of this assumption has been found. An equation similar to (2) in form has been proposed by Sanditov and Bartenev [63]:

$$E_{act} = E_{act\,0} + kT\left(\exp\frac{E_{act\,0} + V_{act}P}{kT} - 1\right). \tag{8}$$

For small values of P, equation (8) becomes the ordinary linear equation $E_{act} = E_{act\,0} + PV_{act}$. According to Doolittle [64], at high pressures viscosity increases more rapidly than by an exponential law due to the decrease in the free volume in the liquid:

$$\eta = \eta_0\exp\left(\frac{\theta}{V - V_0}\right), \tag{9}$$

where θ is a constant, and V_0 is the volume corresponding to vitrification. The elastic energy model, which provides a fairly good description of the viscosity of metallic melts in the initial pressure range [37], is entirely unsuitable for describing the behavior of organic liquids, since the constant C in equation

(4) changes severalfold in the pressure range in question [37]. There were, however, attempts to modify this model by combining it with the free-volume model of Doolittle [37, 65, 66]. According to Keyes [37],

$$V_{\rm act} = AE_{\rm act}\frac{V}{V - V_0}\,, \qquad (10)$$

with A a constant. According to Bridgman [13], the growth of viscosity by many orders of magnitude and vitrification under pressure are due to the 'jamming' of molecules in liquids — the larger the molecules and the more complex their shape, the lower the pressure at which such jamming occurs.

Data on the viscosity of rare-gas liquids have usually been analyzed in the framework of the exactly solvable models of hard and soft spheres [53–55]. Good agreement with experimental results has been achieved at high temperatures, where the liquid density is lower than the density near the triple point, and the equations describing dense gases are correct with a good accuracy [54]. At temperatures close to the melting curve, where a substantial increase in density under pressure is observed, the models provide only a qualitative description of the increase in viscosity with pressure [14, 16]. When applied formally to rare-gas liquids, the activation approach yields $V_{\rm act} \sim 0.25V_{\rm at}$.

Summing up, we can draw the conclusion that there are no universal approaches to the problem of describing the behavior of viscosity for different types of substances under pressure. The model in which the viscosity is constant along the melting curve contradicts the experimental data for molecular liquids [12, 13] and rare-gas liquids [67]. The requirement that the viscosity along isochores be constant is also only approximate and is met only for densities below the melt density at the triple point [14]. Note that within the framework of an activation dependence (2) of the Arrhenius type, the constancy of viscosity along the melting curve means that the activation volume is very small (several percent of the atomic volume) and decreases as the pressure grows, while the constancy of viscosity along an isochore means that the activation volume is large, $(0.2-0.4V_{\rm at})$, and increases with pressure. Typical data for molecular liquids and rare-gas liquids qualitatively agree quite well with the second approach (see Figs 1 and 2), while for liquid metals the narrow range of pressures investigated makes it impossible to draw an unambiguous conclusion about the validity of various empirical models in the high-pressure range.

2.3 Viscosity of liquid iron and the Earth's structure

The viscosity of liquid iron under pressure is probably the most interesting question since, as noted earlier, it is assumed that the outer part of the Earth's core (Fig. 3) consists of an iron-based melt. At present it is generally assumed that the inner part of the Earth's core (see Fig. 3) is crystalline [7]. Another model proposed was a porous crystalline inner core impregnated with a metallic melt of a somewhat different structure with a dendritic inner–outer core boundary [68]. Lately it has been discovered that the inner core of the Earth is anisotropic [69] and precesses [70–72]. Today the inner solid core of the Earth is also considered to be non-uniform and to consist of an outer non-precessing part and an inner precessing part [73], although such ideas do not agree very well with the hypothesis of a crystalline inner core.

The density of iron melt in the conditions at the Earth's core is 10.5–13.5 g cm^{-3}, which is 1.5 to 2 times higher than

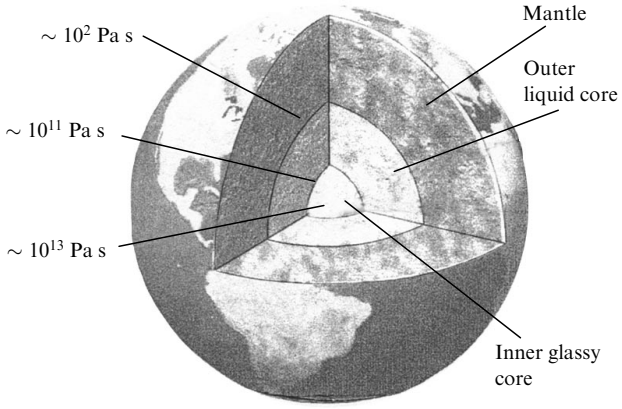

Figure 3. Earth's structure. The assumed states of Earth's inner and outer cores and the typical values of viscosity at the mantle boundary, between the outer and inner cores, and at the center of the core are given on the basis of the analysis in the present review.

the density of liquid iron under normal pressure. The viscosity of the melt in the Earth's core largely determines the heat and mass transfer, the magnetic field and the natural oscillations of the Earth, the emergence and motion of mass fluxes at the core–mantle boundary, the formation of deposits, etc. [7]. Various indirect experiments yield a record-breaking spread in the estimated values of the viscosity of the outer core from 10^{-3} to 10^{11} Pa s [7], while the most accurate estimates based on measurements of the attenuation of seismic waves yield values in the 10^4-10^8 Pa s range [7, 74–76], which is 6 to 10 orders of magnitude greater than the viscosity of iron melt under normal pressure. At the same time, the models we have just discussed imply that the viscosity of iron melt in the conditions at the Earth's core is close to the viscosity of liquid iron under normal pressure near the melting point [7, 23], i.e. $\eta \sim 10^{-2}$ Pa s. Unfortunately, the empirical expressions (3), (4), and (6) only provide a good description of the behavior of the viscosity of metallic melts for small variations in density, which is surely not the case for the Earth's core. Recently Vocadlo et al. [77], de Wijs et al. [78], and Alfe and Gillan [79, 80] attempted to obtain an estimate for the viscosity of iron melt under megabar pressures by numerical methods. They also arrived at small viscosity values, $\eta \sim 10^{-2}$ Pa s. Note that the different values for the viscosity of the liquid core correspond to two markedly different types of melt circulation. When the viscosity is $\eta \sim 10^{-3}-10^{1}$ Pa s, small-scale turbulent circulations similar to atmospheric circulations are observed, but when $\eta \sim 10^{3}-10^{10}$ Pa s, global laminar circulations similar to those in the world's oceans are observed [75]. The different models for the dynamics of the Earth's liquid core correspond to markedly different concepts of the emergence and preservation of the Earth's magnetic field [7, 75, 81, 82].

Thus, the study of the behavior of the viscosity of metal melts (especially of iron melt) and the construction of theoretical models that provide a meaningful description of the viscosity of liquids in a broad range of densities and pressures are extremely important tasks. Most interesting is the study of the viscosity of metallic melts near the melting curve. The thing is that the interiors of many celestial bodies (Earth-like planets, white dwarfs, etc.) are in a partially molten and partially crystallized state, i.e. in these objects the P, T conditions that are realized are close to the melting

points $T_m(P)$ of the corresponding substances (Fig. 4 schematically depicts the phase diagram of iron and the inner conditions of the Earth's core). Obviously, studies of the viscosity of the melts of these substances along the melting curve may provide an estimate for the viscosity of the interiors of celestial bodies. Here it becomes possible to establish the extent to which the empirical formulas (3), (4), and (6) are valid.

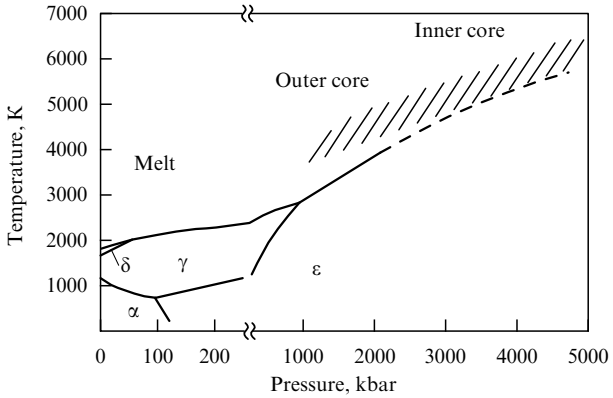

Figure 4. Phase diagram of iron according to Boehler [8] and Tonkov [58] with extrapolation of the melting curve (dashed line). The hatched section denotes the range of temperatures and pressures characteristic of the Earth's core.

3. Measuring the viscosity of melts along the melting curve

3.1 Method of determining viscosity

The fact that the melting temperatures of most metals are high (e.g. for iron $T_m = 1811$ K at $P = 0$ and $T_m \sim 5000$ K at $P = 3$Mbar) makes it very difficult to measure the viscosities of melts directly. However, a method that has proved to be very effective is that of estimating the viscosity variations. This method is based on studying the average grain size in samples that have crystallized under different pressures [31, 34]. For high cooling rates $T > 10^3$ K s^{-1}, and sufficiently pure melts, the condition for homogeneous nucleation and growth of crystal grains (crystallites) is met [34, 83]. Here it appears that the pressure dependence of the relative supercooling of the melt, $\Delta T/T_m$, is determined primarily by the pressure dependence of the surface tension at the melt – crystal boundary, while the grain size is chiefly related to the value of the diffusion coefficient or viscosity.

When nucleation is homogeneous, the nucleation rate I is given by the expression

$$I = nv \exp\left(-\frac{\alpha\sigma^3 V_s^2 T_m^2}{H_m^2 \Delta T^2 kT}\right) \exp\left(-\frac{\Delta G'}{kT}\right), \quad (11)$$

where n is the atomic concentration, v is the characteristic frequency (of the order of the Debye frequency), α is a numerical coefficient, V_s is the molar volume, H_m is the enthalpy of melting, σ is the surface tension coefficient at the grain – melt boundary, k is Boltzmann's constant, and $\Delta G'$ is the energy of activation for the diffusion of atoms in the nucleation process. The crystal growth rate U can be expressed as follows:

$$U = Ca_0 v\left[1 - \exp\left(-\frac{H_m \Delta T}{T_m kT}\right)\right] \exp\left(-\frac{\Delta G''}{kT}\right), \quad (12)$$

where C is a numerical constant, a_0 is the characteristic distance (of the order of the interatomic distance), and $\Delta G''$ is the activation energy for the diffusion of atoms in the process of crystal growth in the melt. Usually, for metals both quantities, $\Delta G'$ and $\Delta G''$, are close in value to E_{act}, which determines the viscosity and diffusion in melts [83].

The average grain size d in a crystallized sample can be estimated by the formula

$$d \sim Ut, \quad (13)$$

where t is the time of crystal growth. On the other hand, the condition for the completion of the growth process yields another estimate for t:

$$It(Ut)^3 \sim 1. \quad (14)$$

Combining (13) and (14), we get

$$d \sim \left(\frac{U}{I}\right)^{1/4}. \quad (15)$$

For cooling rates in the $10^2 - 10^5$ K s^{-1} range, the supercooling ΔT of metallic melts usually amounts to $(0.05 - 0.2)T_m$, i.e. $\Delta T/T_m \ll 1$, with the exception of melts with high viscosity, where supercooling may become significant, $\Delta T \sim (0.3 - 0.4)T_m$. The cooling time $\tau \sim \Delta T/\dot{T}$. Crystallization occurs near the temperature $T = T_m - \Delta T$. The temperature interval $\Delta\widetilde{T}$ within which crystallization occurs under constant cooling can be found from the condition that the intensity of formation of the crystalline phase, determined by the quantity $U^3 I$ [31, 32, 83], changes severalfold:

$$\Delta\widetilde{T} \sim \frac{H_m^2}{\sigma^3 V_s^2} \frac{T^2 \Delta T^4}{(4TT_m - 3T^2 - T_m^2)T_m^2}. \quad (16)$$

For $\Delta T \ll T_m$ we have

$$\Delta\widetilde{T} \sim \Delta T\left(\frac{\Delta T}{T_m}\right)^2. \quad (17)$$

Estimates made for real metallic melts show that $\Delta\widetilde{T}$ is usually much smaller than ΔT (at $T_m \sim 1000$ K we have $\Delta T \sim 100$ K and $\Delta\widetilde{T} \sim 10$ K).

Since the crystallization time $t \sim \Delta\widetilde{T}/\dot{T}$, combining (13) and (17) we get

$$d \approx C\Delta T\left(\frac{\Delta T}{T_m}\right)^2 \exp\left(\frac{-E_{act}}{kT}\right), \quad (18)$$

where C depends on σ, V_s, H_m, and $\dot{T}$. Experiments have shown that for a fixed cooling rate the pre-exponential factor $C\Delta T(\Delta T/T_m)^2$ usually varies with pressure 5 to 10 times more weakly than $\exp(-E_{act}/kT)$ [83], i.e. $d \sim \exp(-E_{act}/kT)$. Hence to a first approximation the relative variation with pressure of the grain size in crystallized samples in the stability region of one of the phases corresponds to the relative variation with pressure of the viscosity of the melt at the crystallization temperature:

$$d \sim D \sim \frac{1}{\eta}. \quad (19)$$

Thus, the dependence of the grain size on the pressure under which the quenching from the melt took place is determined primarily by the pressure dependence of the supercooled melt at a temperature near the melting point (at $T = T_m - \Delta T$). In the same way it can be shown that the size of the relative supercooling under pressure is determined primarily by the pressure dependence of the surface tension, which can be found by solving equations (15) and (18) simultaneously [31, 34, 83].

Hence quantitative information about variations of viscosity and surface tension under pressure can be obtained by measuring d and ΔT in conditions of fast ($\geqslant 10^3$ K s^{-1}) quenching from the melt at different pressures. In the present review we mainly discuss the pressure dependence of viscosity. Note that within the empirical models (3), (4), and (6) the size of the grains in samples that crystallized under different pressures must be almost the same.

3.2 Experimental studies of the viscosity of metallic melts

At this point it appears advisable to briefly discuss some experimental details. A pressure in the 10–95 kbar range was created in a chamber of the 'toroid' type [84]. The samples were cylinders 2 mm high and 2 mm in diameter pressed from 99.99%-purity Fe, Cu, In, and Pb powders. They were placed in an ampule made from single-crystal NaCl. The measured average rate of cooling of the melt near the melting point coincides to a high accuracy with the value estimated from heat conduction equations and ranges from 10^3 to 5×10^3 K s^{-1} for different materials. As the pressure was increased from 10 to 95 kbar, the average rate of sample cooling was found to increase by only 15–40%. The size and morphology of the crystal grains were studied with the optical microscope NEOPHOT and the electron scanning microscope Stereoscan MK2. Cleavages prepared in liquid nitrogen and polished microsections treated with appropriate etchants were also studied.

The size and morphology of the grains that form as a result of crystallization of melts were studied for four metals: Pb, In, Cu, and Fe (the examples are depicted in Figs 5 and 6). Here the supercooling pressure dependence obtained for the more easily fusible melts of Pb and In made it possible to estimate the pressure dependence of the surface tension [31, 35]. Crystals of Pb, In, and Cu do not undergo phase transitions in the pressure range in question [58]. Multiple melting–quenching cycles in samples of all the metals did not reveal appreciable variations in the crystallite size, which agrees with the assumption of homogeneous nucleation and of the absence of any effect on the size and morphology of the grains from transitions in the solid state.

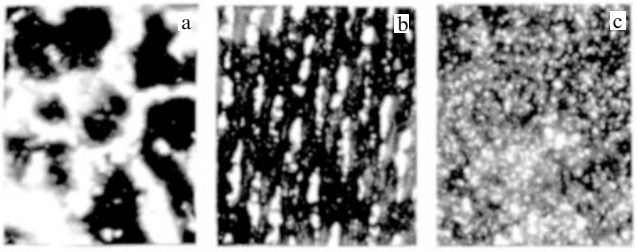

Figure 5. Typical micrographs of microsections of copper samples quenched from the melt at high pressures: $P = 20$ kbar (a), 50 kbar (b), and 80 kbar (c). The size of the fields is 100 μm by 80 μm.

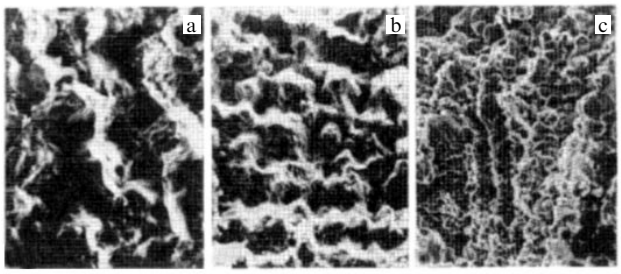

Figure 6. Typical micrographs of cleavages of iron samples quenched from the melt at high pressures: $P = 56$ kbar (a), 72 kbar (b), and 93 kbar (c). The size of the fields is 190 μm by 140 μm.

There is one complication involving iron samples: in the temperature range from room temperature to the melting point for $P < 50$ kbar, the iron crystals undergo phase transitions, $\alpha-\gamma$ and $\gamma-\delta$, while for $P > 50$ kbar there is only one phase transition, $\alpha-\gamma$ (see Fig. 4) [58]. Theoretically, these transitions may change the size and morphology of the grains, but the small discontinuity in volume in these transformations (1% and 0.5%, respectively) and the high plasticity of iron crystals suggest that the grains do not become smaller in the solid state.

The grains in the sample under investigation had a rounded, columnar, and dendritic morphology (see Figs 5 and 6) with a texture corresponding to the temperature gradient in cooling, i.e. along the axis of the cylindrical sample [36]. The pressure curves representing the pressure dependence of the average grain size are depicted in Fig. 7. The variation in the viscosity of the iron melt under pressures ranging from 56 kbar to 95 kbar corresponds to an effective activation volume in equation (2) of $V_{act} \sim (0.35-0.4)V_{at}$. The discontinuity in the absolute values of the grain size in iron polycrystals is probably due to the fact that the values of the surface tension of the melt with respect to the δ- and γ-phases are different. For the other melts, Pb, In, and Cu, it was also established that the pressure curves in the pressure range from 20 to 80 kbar correspond to an effective activation volume $V_{act} \sim (0.2-0.35)V_{at}$.

The fact that in the pressure range under investigation the size of the grains of the metals decreases severalfold (see

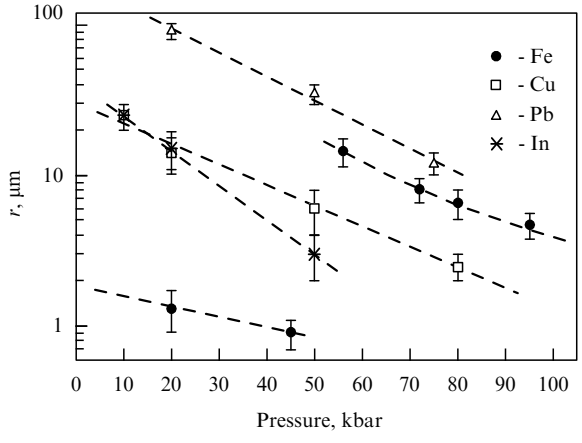

Figure 7. Pressure dependence of the average grain size for metal samples quenched. In the case of iron there is a discontinuity in d related to the phase transition in iron at high pressure.

Fig. 7) indicates that the viscosity of the corresponding melts increases severalfold near the melting curve. The results shed new light on a whole range of problems related to the behavior of melts under pressure. The reader will recall that the models (3), (4), and (6) predict a grain size that is independent of the solidification pressure, a behavior that completely contradicts the experimental data. Notwithstanding the more complicated phase diagram, we believe that the studies of solidification of liquid iron under pressure are very important for reasons discussed in the Introduction. Hence in what follows, when discussing the results, we focus on the data obtained for iron.

4. Universal viscosity behavior in melts under pressure

The data gathered for iron [35] and the results obtained for Cu, In, and Pb [31, 35] (see Fig. 7) contradict the assumption that viscosity is constant along the melting curve. At the same time, they probably indicate the presence of general laws governing the behavior of metallic melts under pressure. This is especially true of the growth of viscosity along the melting curve. At present there is no theoretical proof that the viscosity of melts of different substances, and even more so of different classes of substances, obeys universal laws. Nevertheless, we will see below that there are reasons to believe that such universal laws may exist due to the general features of the central interaction (repulsion) of different atoms when the substance is compressed. Let us consider what conclusions can be drawn from the assumption that the growth of the viscosity of melts under isothermal compression is a universal property.

It is natural to associate the growth in the viscosity of melts with the activation law (2). Here we can assume that, just as in molecular organic liquids, the effective activation volume in metallic melts increases rapidly with pressure from $0.05V_{at}$ at $P < 10$ kbar to $(0.2-0.4)V_{at}$ at $P > 30$ kbar (see Fig. 2). Note that for rare-gas liquids, $V_{act} \sim 0.25V_{at}$ already at $P > 5$ kbar. That is, for all liquids, starting from certain pressures (several kilobars for organic liquids and several tens of kilobars for metal melts) the behavior of viscosity under pressure is universal (see Fig. 2), with the same activation volumes, $\sim (0.2-0.4)V_{at}$, as in crystals.

On the basis of such values for the effective activation volume for metal melts, one can expect an exponential growth of viscosity by 5 to 15 orders of magnitude already in the megabar pressure range, with the result that a state with the viscosity of glass can be achieved. Therefore, it is natural to assume that the data of shock-wave experiments [44–47] indicating that viscosity increases by several orders of magnitude are correct, since they yield the same values for the activation volume, $\sim (0.2-0.4)V_{at}$. Similar variations in the viscosity of organic liquids occur at pressures that are ten times lower (about 100 kbar). This happens simply because of the large volume of the corresponding molecules in comparison with the volume of metal atoms.

Up to this point we have considered only the equilibrium isothermal build-up of viscosity of liquid iron, with the values reaching those characteristic of glass, which actually means that the melt transforms into a glass. The possibility of vitrification of the melt in the supercooled state on quenching is also determined primarily by the melt's viscosity [83, 85]. If we take our estimates of the viscosity of liquid iron under pressure as the starting point, it appears that at cooling rates in the 10^3-10^7 K s^{-1} range crystallization of iron melt can be avoided during solidification at pressures starting from the 0.7–1.5 Mbar range. Earlier one of the authors of the present review obtained similar estimates, ~ 0.5 Mbar, in discussing vitrification during the rapid cooling of Pb and In melts [31, 35]. The validity of these estimates is open to direct experimental verification: after being melted under pressures in the megabar range, samples of solid iron and other metals should acquire an amorphous structure as a result of the solidification process.

5. Transition to the 'solid' diffusion regime in melts under high compression

What are the reasons at the microscopic level for viscosity to change under pressure? While it is natural to relate the increase in the viscosity of melts initiated by a drop in temperature (as well as vitrification of a supercooled melt) with the freezing-up of atomic motion, the microscopic picture of the diffusion processes is more complicated when pressure is increased isothermally. It is a well-known fact that the activation law provides a good description of the temperature dependence of the diffusion coefficients for both solids and liquids. The reason for this is that the diffusion processes are determined by the fluctuation production of mobile activated states (vacancies, interstitial atoms, or complexes consisting of vacancies). For most solids and melts the corresponding activation energies increase with pressure. To the first approximation, the variation in the activation energy can be assumed to be proportional to pressure [see equation (2)], with the respective proportionality factor being the activation volume.

From this point of view, the exponential increase with pressure of the viscosity of metal melts under isothermal compression and the exponential decrease in the diffusion coefficients of the respective crystals are unquestionable. In some cases the activation volume has a definite physical meaning and is determined primarily by the geometric characteristics of the activated states participating in the diffusion process. In other cases the activation energy is a non-linear function of pressure, with the result that the activation volume is not a constant quantity with a definite physical meaning. Such behavior can be observed, for example, when one mechanism is replaced by another.

It is also natural to link the increase in the activation volume for the viscosity of melts under pressure with a change in the atomic transport mechanism. The reason the effective activation volumes for the pressure dependence of the viscosity of liquids at low pressures is small is that there is a large 'free' volume in the melt, amounting to roughly 5 to 10% of the total volume [37, 60]. The diffusion activation energy is actually related only to the activation energy of vacancy displacement, while no energy is needed to generate vacancies since there are a lot of them in the melt. At high pressures, however, the situation changes dramatically: the free volume in a liquid rapidly decreases (as well as the volume discontinuity in melting) and, starting from certain pressures, there are practically no thermodynamically equilibrium vacancies, neither in crystals nor in liquids. In solids at temperatures in the 500–1000 K range, the corresponding range for the 'closure' of vacancies is 30 to 100 kbar, while in metallic melts at $T \sim 1500-4000$ K, there are no vacancies at $P > 150-500$ kbar (for molecular organic liquids the pressure is ten times lower). At higher pressures the free

volume in melts that is produced during melting ($\sim 1\%$) is distributed not in the form of vacancies and excess interatomic space (microcavities) but 'spreads' over regions encompassing tens and hundreds of atoms (Fig. 8) due to the fluctuations of the lengths of and angles between bonds, as in amorphous solids. An analysis of the experimental data [12] shows that not only does the activation energy E_{act} increase in organic liquids subjected to pressure, but also the pre-exponential factor η_0 in equation (2) drops. This is also an indication of a transition to the 'solid' diffusion regime, since the pre-exponential factor η_0 in glasses and crystals is usually one to two orders of magnitude smaller than in the respective melts [22, 86].

The vacancy mechanism of diffusion in solids and melts is replaced, under pressure, by diffusion of atoms over interstitial sites [13, 51], with a large number of atoms involved in a single diffusion act owing to stress relaxation. This was first noticed by Bridgman [13], who attributed the anomalously fast growth of viscosity with pressure in organic liquids to the rapid increase in the effective size of the activation complexes (see Fig. 8) determining diffusion processes. It is difficult to make quantitative estimates of the effective activation volume in the diffusion of atoms in a compressed substance over interstitial sites because one must carefully account for the relaxation of the generated stresses on the atomic level. An additional difficulty emerges when melts are involved because one must accurately take into account the fluctuations of the local structural characteristics. A simple estimate of the energy needed to generate a vacancy yields $V_{act} \sim (0.7-1)V_{at}$ [37, 51, 52, 87]. The reader will recall that most calculations of the diffusion in crystals yield $V_{act} \sim (0.4-1)V_{at}$.

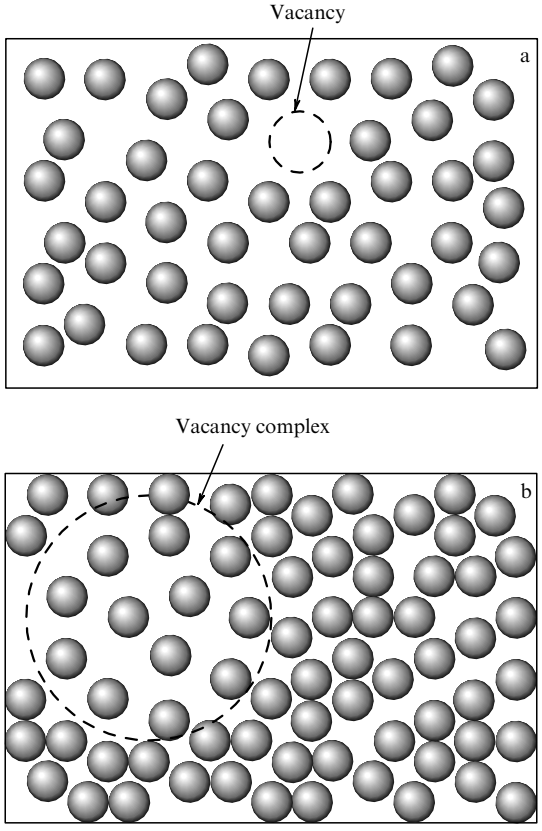

Figure 8. In normal conditions the free volume in melts is largely related to the activation of vacancies (a), while at high pressure it is related to multiatomic vacancy complexes (b). As pressure grows, the vacancy mechanism of diffusion is replaced by diffusion of atoms over interstitial sites and a cooperative mechanism for the motion of atoms in vacancy complexes.

The diffusion of atoms over interstitial sites probably corresponds to smaller values of V_{act}. An appropriate estimate of V_{act} can be made in the continuum approximation. The maximum shear stress that a condensed substance can sustain on the interatomic-distance scale is $\sigma \sim G/(2\pi)$ [88], where G is the effective shear modulus, which in the melt is close (over 'distance of' order of interatomic spacing) to the corresponding value for the solid [89]. When pressure is applied, the shear modulus increases linearly (to the first approximation) with pressure, $G \sim G_0 + \alpha P$, where $\alpha \sim 1-2$ [90], and when $P > G_0$, we can assume that $G \sim \alpha P$, i.e $\sigma \sim \alpha P/(2\pi)$. The energy related to these stresses is $E \sim \sigma V_{at} \sim (\alpha P/2\pi)V_{at}$, i.e. $V_{act} \sim (\alpha/2\pi)V_{at} \sim (0.15-0.3)V_{at}$. More accurate estimates of V_{act} with allowance for the realistic interatomic interaction require computer calculations from first principles.

6. Evolution of the viscosity of melts along the melting curve

The behavior of viscosity along the melting curve merits separate discussion. It is much more difficult to examine the behavior of viscosity when variations of both pressure and temperature are taken into account simultaneously. As shown in Sections 3.2 and 4, the viscosity of metallic melts grows substantially along the melting curve. Obviously, the assumption that the viscosity of metallic liquids along the melting curve is constant (made by Poirier [23]) is only approximately true in the initial pressure range. For instance, for liquid mercury the lines of constant viscosity in the P, T plane have a slope of $(7.5-8)$ K kbar^{-1} [28], while the slope of mercury's melting curve is roughly 5 K kbar^{-1} [58] (Fig. 9). Note that for iron the assumption of the constancy of viscosity along the melting curve leads to a 'non-physical' result: as the pressure grows, the small quantity V_{act} decreases still further, from $0.05V_{at}$ at $P = 0$ to $0.02V_{at}$ at $P = 3$ Mbar. Examples of other liquids (rare-gas liquids [67] and organic substances [13, 15, 19]) also suggest that along the melting curve viscosity increases rapidly with pressure and this increase is accompanied by an increase in the effective activation volume.

The assumption that the viscosity of liquids is constant along isochores is also not quite true. An analysis of the experimental data for melts of different nature (metals, organic liquids, and rare-gas liquids) shows that the viscosity slowly decreases along isochores as the pressure grows. The lines of constant viscosity can be described by the equation $\rho^n T^{-1} = \text{const}$, where the data of Trappeniers et al. [16] and Bridgman [28] yield the following: $n \sim 8 \pm 1$ for liquid mercury and $n \sim 7 \pm 2$ for liquid argon (see Fig. 9).

If we assume that the pressure dependence of viscosity of the Arrhenius type is valid at high pressures, the condition of the constancy of viscosity yields $(E_{act\,0} + PV_{act})/T = \text{const}$, which means that $PV_{at}/T = \text{const}$ if we ignore $E_{act\,0}$ and if we assume that V_{act} is proportional to V_{at}. For most metals

$$P \sim \rho^{4-5}, \tag{20}$$

since the bulk modulus B, defined as $B = -\rho(\partial P/\partial\rho)$, in most metal increases linearly with pressure, $B = B_0 + \alpha P$, and

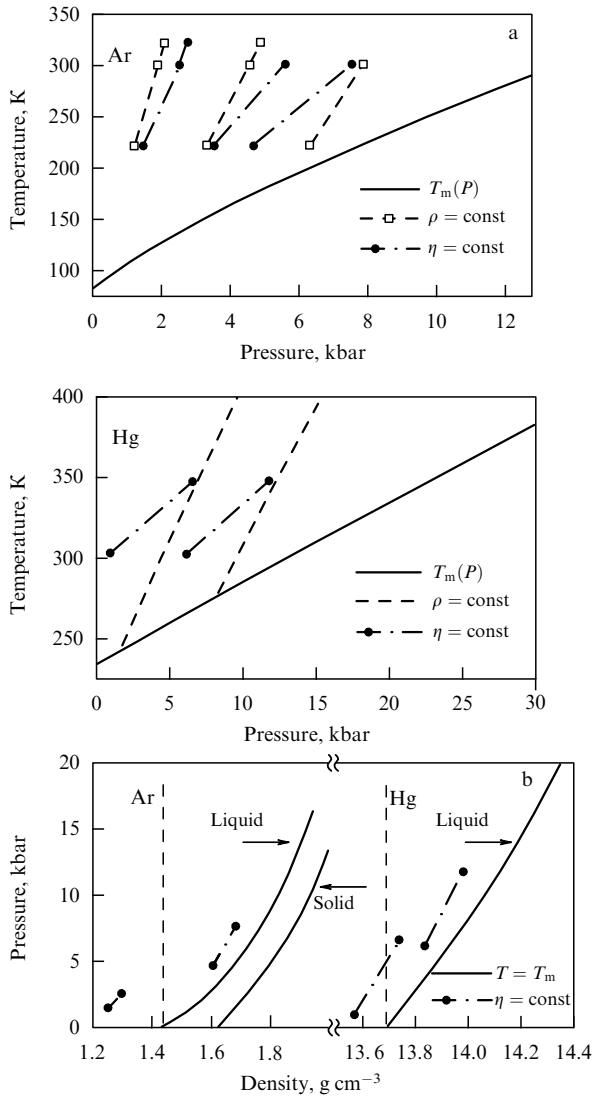

Figure 9. Relative position of constant-viscosity lines ($\eta = \text{const}$), isochores ($\rho = \text{const}$), and melting curves ($T = T_m$) for mercury and argon in the P, T (a) and ρ, P (b) planes. The variation in the density of mercury has been calculated from the coefficients of thermal expansion and compressibility [49]. The viscosity of mercury under pressure is known at 303 and 348 K [28]. The data on the density and viscosity of liquid argon have been taken from Ref. [16] for two temperatures: 223 and 301 K. The melting curves for Hg and Ar and the discontinuity of the volume in melting of argon have been taken from Refs. [58, 91] and Ref. [92], respectively.

$\alpha \sim 5$ [90]. With allowance for the fact that $V_{at} \sim 1/\rho$, the condition for the constancy of viscosity means that

$$\rho^{3-4} T^{-1} \approx \text{const}\,, \tag{21}$$

which exactly corresponds to the slow decrease of viscosity along isochores as the temperature increases.

The following condition is met along the melting curve for iron under megabar pressures [8, 10]:

$$T_m \sim \rho^{1-1.5}\,. \tag{22}$$

Correspondingly, for viscosity along the melting curve we obtain

$$\eta \sim \exp(C_1 \rho^{1.5-2.5}) \sim \exp(C_2 P^{0.4-0.7})\,, \tag{23}$$

where C_1 and C_2 are constants. Thus, the formal reason for the rapid buildup in the viscosity of metal melts along the melting curve is that the $T_m(\rho)$ dependence is weak compared to the strong $P(\rho)$ dependence [see equations (20) and (22)].

The Clausius – Clapeyron equation yields

$$T_m(P) \sim T_{m0} + \int \frac{\Delta V_m}{\Delta S_m}\, dP\,, \tag{24}$$

where ΔV_m and ΔS_m are, respectively, the discontinuities of pressure and entropy in melting. The entropy jump at melting changes only slightly with pressure (usually from 1 – 1.5 to 0.8 – 1 [93]). For high pressures, where $T_m \gg T_{m0}$, equation (24) yields

$$T_m \sim \overline{\Delta V_m} P \sim \Delta V_m P\,, \tag{25}$$

where $\overline{\Delta V_m}$ is the volume jump at melting averaged over the pressure interval under consideration. This quantity is determined primarily by the volume discontinuity ΔV_m at the highest pressure, while ΔS_m is close to unity.

Combining (2) and (25) while allowing for the fact that under pressure $E_{act\,0} \ll P V_{act}$, we arrive at the following expression for the viscosity along the melting curve:

$$\eta \sim \exp\left(\frac{V_{act}}{\Delta V_m}\right) \sim \exp\left(\frac{V_{act}/V_{at}}{\Delta V_m/V_{at}}\right). \tag{26}$$

For metals, the relative discontinuity of the volume in melting under pressure tends to zero or to a very small quantity that amounts to several tenths or even hundredths of one percent [93], while the ratio V_{act}/V_{at} probably tends to a finite quantity of about 0.2 – 0.4. As a result, the viscosity of liquid metals along the melting curve can formally grow without limit with pressure, in accordance with (26). For rare-gas liquids, the relative discontinuity of the volume in melting under pressure tends to a finite quantity of about 0.03 [93]. Hence for rare-gas liquids the maximum increase of viscosity along the melting curve amounts to three to five orders of magnitude.

The difference in the behavior of the relative discontinuity of the volume in melting under pressure for metals and rare-gas solids is due to the difference in the interatomic interaction potentials. The discontinuity of the volume in melting diminishes as the repulsive part of the potential softens. For a system of particles interacting by the $U \sim 1/r^n$ law, $\Delta V_m/V_{at} \approx 0.1$ at $n = \infty$ (hard spheres), $\Delta V_m/V_{at} \approx 0.04$ at $n = 12$, $\Delta V_m/V_{at} \approx 0.01$ at $n = 6$, and $\Delta V_m/V_{at} \approx 0.005$ at $n = 4$ [94]. In metals the repulsive potential is softer (i.e. it is described by the dependence $1/r^n$ with a smaller n) than in rare-gas solids, which leads to smaller values of $\Delta V_m/V_{at}$. Moreover, in metals $\Delta V_m/V_{at}$ can, at least in principle, decrease to zero under compression. The melting point and hence the discontinuity of the volume in melting are determined by the difference in the structure-dependent contributions to the energy. In the high-compression limit the Coulomb contribution $T_m \sim \rho^{1/3}$ is the primary factor for metals [4, 11, 95]. Considering that for metals under extremely high compression the pressure dependence of the volume is determined primarily by the Fermi structure-independent contribution of electrons to the energy, $V_{at} \sim 1/\rho \sim P^{-3/5}$ [88, 96], we have $T_m \sim \rho^{1/3} \sim P^{1/5}$. Since from (25) it follows that $\Delta V_m \sim T_m/P \sim P^{-4/5}$, we arrive at the expression

$$\frac{\Delta V_m}{V_{at}} \sim P^{-1/5}\,, \tag{27}$$

which supports the tendency of the relative discontinuity of the volume in the melting of metals to zero. The dependence of $\Delta V_m/V_{at}$ on P is weak, and the values of $\Delta V_m/V_{at}$ that can be attained in metals at $P \sim 1-100$ Mbar amount to 0.1–0.5%; this, however, is sufficient for the viscosity to become as high as in glasses, in accordance with (26).

When the interatomic interaction is described by a pair central potential, e.g. for rare-gas solids, the relative discontinuity of the volume in melting tends to a finite quantity under high compression, since the same structure-dependent part of the energy determines the pressure dependences of the atomic volume and of the discontinuity of the volume in melting. Recent experimental studies of the melting curves of different substances in the megabar pressure range [8, 97] fully corroborate the conclusion that in metals $\Delta V_m/V_{at}$ decreases under compression more rapidly than in non-metals and that the melting curves of metals flatten, as pressure grows.

In the high-compression limit, the value of the relative activation volume for diffusion, V_{act}/V_{at}, is finite for both van der Waals substances and metals because of the presence of a strong interatomic repulsive potential and of a hard atomic core, which leads to a high activation energy for the motion of atoms over interstitial sites. In the limit of extremely high compressions, $P \gg 100$ Mbar, the metal becomes a crystalline plasma of bare ions and electrons. In this case the presence of a soft Coulomb ion–ion repulsive potential and the absence of an atomic core must lead to a reduction in V_{act}/V_{at} to zero. Indeed, in this case $E_{act} \sim \rho^{1/3}$, i.e. $V_{act} \sim \rho^{1/3}/P \sim P^{-4/5}$, or

$$\frac{V_{act}}{V_{at}} \sim P^{-1/5} \tag{28}$$

tends to zero by the same law as $\Delta V_m/V_{at}$ [see equation (27)]. As a result, the viscosity of such plasma near the melting curve, e. g. in white dwarfs, probably remains not very high; note that the data from computer simulations using the molecular dynamics method also predict a slow increase in the viscosity of the electron–ion plasma under high compression along the melting curve [95, 98, 99].

Thus, the effect of the limitless increase in viscosity along the melting curve manifests itself only in substances with a sufficiently soft interatomic repulsive potential (e.g. metals) that are subjected to certain degrees of compression (the 1–100 Mbar pressure range corresponding to compression by a considerable factor along the melting curve). Here the compression ratio is largely determined by the kinetic Fermi and ion–ion contributions to the energy, while the structure-dependent part of the cohesive energy and hence the melting temperature and the volume jump at melting are determined primarily by the Coulomb part of the interaction. At the same time, the activation energy of the diffusion of atoms is determined by the repulsive part of the interatomic potential and the presence of a core of inner electrons. In this case the activation volume constitutes a sizable part of the atomic volume, and the relative discontinuity of the volume in melting may become very small.

Note that formally the above discussion of the melting temperature under pressure does not quite correspond to the common approach, according to which melting is determined primarily by the repulsive part of the potential. The thing is that the common approach is justified only for systems with hard repulsion in the interatomic pair potentials (a large n in the $1/r^n$ dependence). In the case of metals, however, the contribution of the attractive part of the effective interatomic potential to the melting temperature is not small at all pressures, and under very high compression this contribution becomes the principal one [93].

7. Viscosity of metallic melts in the interiors of the Earth and other planets

The extrapolation of the experimental data on the viscosity of melts and the theoretical ideas discussed above make it possible to analyze the behavior of the Earth's liquid core. If we take the estimate for V_{act} obtained above as the starting point, we see that the viscosity of iron melt in the conditions at the Earth's core must be 5 to 12 orders of magnitude higher than under normal pressure: roughly $\sim 10^1-10^3$ Pa s near the core–mantle boundary and roughly $\sim 10^7-10^{11}$ Pa s near the inner–outer core boundary (see Fig. 3). Thus, estimates of the viscosity in the interior of the Earth based on measurements of the attenuation of seismic waves yield correct results corresponding to the average value of the viscosity in the outer core $\sim 10^3-10^6$ Pa s [7, 74–76]. Recently, Smyle [100] concluded, on the basis of seismic data, that near the inner–outer core boundary the viscosity of the melt may be extremely high ($\sim 10^{11}$ Pa s). Hence there must be global non-turbulent circulation in the liquid core [76]. Laminar circulation, in contrast to turbulent circulation, may lead to a non-adiabatic temperature distribution in the liquid core. Moreover, non-turbulent circulation of the conducting melt in the core would lead to a picture of the emergence and evolution of the Earth's magnetic field entirely different from the generally accepted one [76]. Laminar circulation of the melt in the core must also be taken into account when one analyzes the formation of plumes at the core–mantle boundary [101].

The incorrect estimates of the slow growth of viscosity with pressure made by Poirier [23] for liquid iron were due to the unjustified extrapolation of equations (3), (4), and (6), which are not general enough to describe large compressions. The reasons for the slow growth of the viscosity of iron melt obtained in molecular-dynamics simulations by Vocadlo et al. [77] and de Wijs et al. [78] are not entirely clear. As is known, the pseudopotentials used by the researchers predict the thermodynamic properties of the melt fairly accurately but only lately they have been used to calculate the coefficients of diffusion under pressure. The reader will also recall that in the viscous region the Stokes–Einstein relationship becomes invalid and an increase of viscosity of 8 to 11 orders of magnitude may correspond to a decrease in the values of the calculated diffusion coefficients by only 2 to 3 orders of magnitude [24–27].

The possibility of viscosity becoming as high as $\sim 10^{10}-10^{11}$ Pa s at the inner–outer core boundary means that in relation to seismic vibrations with a typical probing frequency of 1 Hz the melt behaves as a solid, since the characteristic relaxation time $\tau \sim \eta/G$ (where G is the shear modulus of the medium) becomes comparable with the reciprocal frequency of the seismic vibrations. As noted in Section 2.1, near the vitrification pressure the viscosity grows faster than exponentially (critical behavior is observed) [19]. Hence the growth in the viscosity of iron melt from 10^4-10^7 to 10^{11} Pa s may occur within a fairly narrow range of pressures and, accordingly, of depth in the core. In view of these estimates, there is reason to believe that the old hypothesis of a 'glassy' state of the Earth's inner core [7, 102] will have a promising second life.

For a long time after the discovery of the anomalous increase in the velocity of longitudinal waves in the Earth's inner core, the hypothesis that the Earth's core is a visco-elastic body with viscosity increasing in the inner part up to values characteristic of glass existed parallel to the hypothesis that the Earth's inner core has a crystalline structure [5, 102]. The glassy-core hypothesis was temporarily forgotten at the beginning of the 1960s, when the silicate model of the core lost its credibility [5, 7]. At the time, it was not realized that the vitrification process is universal for different classes of substances, and glassy metals had not yet acquire their rightful place in the class of amorphous substances. Of course, the concept of an inner core consisting of iron-based metallic glass or, to be more exact, of an iron-based melt with a viscosity higher that $> 10^{11}$ Pa s (see Fig. 3) was not even considered.

The return of the hypothesis of the ultraviscous state of the Earth's inner core has shed new light on a number of issues that were unclear at the time. For instance, the Poisson coefficient for the inner core, which was measured by the propagation of longitudinal waves, has a value of roughly 0.44 [7], which is anomalously large for crystalline metals and corresponds to small values of the shear modulus. Note that both the values of the shear modulus calculated by Söderlind et al. [103] and Steinle-Neumann et al. [104] and the extrapolation of the experimental data of Singh et al. [105] and Mao et al. [106] for crystalline iron yield values of G (for the conditions in the inner core) that are 1.5 to 2.5 times larger than the observed values (2–5 Mbar instead of 1.2–1.5 Mbar). At the same time, for metallic glasses the values of the Poisson coefficient $\nu > 0.4$ are quite normal [107]. The reason is that metallic glasses have a shear modulus that is usually 20 to 50% smaller than the respective crystalline prototypes have, while the decrease in the bulk modulus in amorphous metals is much smaller [107–109].

The appreciable difference in the melting points of iron obtained in static [8, 97, 110] and shock-wave [9, 10, 111, 112] experiments can also be understood if we allow for the possible high viscosity of the melt. In this case, in shock-wave experiments there can be substantial overheating of the crystal in relation to the equilibrium melting point. Probably, the estimates made by Boehler for the melting point of iron are correct: $T_m \sim 4800$ K at $P = 3.3$ Mbar [8]. With allowance for the fact that the melting point may be lower due to the possible impurities such as Si, S, O, and H, the melting point in the inner core can be estimated at roughly 3500–4000 K, while the real temperature at the center of the Earth is probably about 5000 K, and at the core–mantle boundary roughly 4000 K [7] (see Fig. 4). Near the inner–outer core boundary the adiabatic buildup of temperature with pressure is about 0.45 K kbar^{-1} [7, 9], while the increase, with pressure, of the melting point for iron is about 0.7 K kbar^{-1} [8, 110]. Due to the high viscosity of the melt in the outer core, the temperature gradient may be substantially larger than the adiabatic gradient (~ 0.6–1 K kbar^{-1}). In other words, the temperature in the Earth's core is probably much higher than the melting point of pure iron and, even more so, of alloys between iron and light elements.

Thus, the evolution of the Earth's core can probably by interpreted not as a gradual crystallization that begins at the center but rather as a 'thickening' of the inner core. New data on the anisotropy [68] and precession [69, 72] of the inner core also find a natural explanation within the concept of the gradual vitrification of the core in the evolution of the Earth and of continuing slow convection in the inner core. Recently, Denisov and Novikov [113] have used data on the rate of precession of the inner core to estimate the average viscosity of the Earth's outer core. The values obtained ($\eta \sim 10^3$ Pa s) exceed the viscosity of iron melt in normal conditions by six orders of magnitude and agree well with our estimates. Note, however, that estimates of the viscosity of the outer core based on the observed values of precession were made earlier and yielded different values for the viscosity, from 10^4 to 10^{-4} Pa s [72].

The problem of the value of the viscosity of the Earth's core is important not only for understanding the Earth's structure but also for solving many problems of celestial mechanics and the motion of the Earth [6]. For instance, the description of the relatively rapid vibrations (nutations) of the Earth's axis depends largely on the absolute values of viscosity of the Earth's interior [114, 115]. The high values of the viscosity of the Earth's outer core can explain the fact that so far no free vibrations of the inner core have been observed. Quantitative information about the viscosity of the Earth's interior is also important for describing the spectrum of forced vibrations of the Earth, the theory of tides, and the effects of the slowing down of the Earth's proper rotation [6].

The high viscosity of different metallic liquids in the megabar pressure range must be taken into account when one examines the behavior of other celestial bodies, too. For instance, the high viscosity of the metallic liquid hydrogen in the interiors of Jupiter and Saturn can explain the anomalously low tidal coefficients of these planets [11]. The viscosity of metallic liquid hydrogen must be taken into account in the analysis of the temperature gradients in the interiors of Jupiter and Saturn and in studies of the magnetic fields of these planets.

8. Ultraviscous state of melts under megabar pressures

Up to this point we have considered the increase in the viscosity of melts under pressure up to values characteristic of glasses. Meanwhile, the problem of the relative position of the glass-transition line and the melting curve under high pressure is interesting in itself.

The pressure and temperature dependences of the viscosity determine the position in the P, T plane of the glass-transition line $T_g(P)$, which formally corresponds to a viscosity of about $\sim 10^{14}$ Pa s (the kinetic definition of the glass-transition line). As is known, from the theoretical point of view vitrification is determined primarily by the repulsive part of the effective pair interatomic potential:

$$\rho^{n/3} T_g = \text{const}\,, \tag{29}$$

where n is the exponent in the repulsive potential [116–118]. For systems with a homogeneous potential function for the interparticle interaction, equation (29) is a direct consequence of the Klein theorem, which states that for a system whose potential energy is a homogeneous function of degree n of the coordinates of the particles, the non-ideal part of the partition function does not depend separately on the volume and temperature but rather is a function of the combined variable $\rho^{n/3}/T$ [93]. For vitrification of molecular liquids it has been established by experiment that $T_g \sim \rho^4$ to a high accuracy, which means that $n = 12$ [118]. The condition $T_g \sim \rho^4$ was also obtained through a molecular-dynamics simulation of

the vitrification of van der Waals liquids [117, 119]. As noted earlier, for metals, it is impossible to introduce an interatomic pair potential in a meaningful manner. Nevertheless, for transition metals, e.g. Fe, the presence of strongly localized d electrons makes it possible to introduce, in a meaningful manner, an effective pair potential that provides a rather good description of the properties of the substances within a broad range of pressures and temperatures [120, 121]. The common approach is to use the '5–8' potential, whose attractive part is $\sim 1/r^5$ and repulsive part is $\sim 1/r^8$ [120, 122]. Hence, for the vitrification point of transition metals we have the following formula:

$$T_g \sim \rho^{8/3}\,, \tag{30}$$

which agrees fairly well with equation (21) for the constant-viscosity lines. The fact that the dependence $T_g(\rho)$ is stronger than $T_m(\rho)$ [cf. (22) and (30)] means that at high pressures the curves $T_g(\rho)$ and $T_m(\rho)$ may intersect (at least in principle) (Fig. 10). Under atmospheric pressure, $T_g \sim (0.3-0.7)T_m$ [123], where the upper values $T_g \sim (0.6-0.7)T_m$ belong to well-glass-forming substances, while the values $T_g \sim (0.3-0.4)T_m$ correspond to the vitrification of metals. When $T_g \sim (0.3-0.4)T_m$, from (22) and (30) it follows that the curves $T_g(P)$ and $T_m(P)$ must intersect under pressure, with the density of the metallic melt increasing along the melting curve by a factor of two to three, which agrees well with the above estimates of the vitrification of the Earth's inner core. The reader will recall that the dependence $T_m(P)$ is weaker than $T_g(P)$ because the vitrification process is largely determined, as is the diffusion process, by the repulsive part of the interatomic potential and by the presence of the hard core consisting of the inner shells, while melting is to a great extent due to the attractive part of the potential [93].

In the hard-sphere model, the vitrification process has been thoroughly studied and is related to achieving a packing index of roughly 0.5 [19, 124]. In the more realistic models of the interatomic interaction used to explain vitrification, the common approach is to introduce the concept of effective hard spheres, after which the analysis is equivalent to that of the hard-sphere model. For metals, the effective hard sphere is assumed to be, to the first approximation, the ion core consisting of the inner electron shells. The ionic radii of metals are 1.5 to 3 times smaller than the atomic radii, i.e. vitrification in this approximation must occur when the density of the melt changes by a factor of 4 to 20. However, a strong repulsive potential leads to a situation in which the radius of the effective hard sphere is much larger than the ionic radius. There are several criteria for determining the radius of the effective hard sphere that yield fairly close results [125]. For molecular organic liquids, the radii of effective hard spheres estimated in this manner make it possible to describe the vitrification of such liquids to a high accuracy [19]. The simplest estimate of the radius of the effective hard sphere for an interatomic pair potential $U(r)$ corresponds to the condition that $U(r) = 0$. Here the real pair potential is replaced by a hard-sphere potential with an appropriate radius and infinitely weak attraction (Fig. 11). In the approximation of a pair $m-n$ potential, the radius of the effective sphere is

$$r_{\text{eff}} \approx r_{\text{at}} \left(\frac{n}{m}\right)^{1/(m-n)}\,. \tag{31}$$

For a potential of the '6–12' type we get $r_{\text{at}}/r_{\text{eff}} \approx 2^{1/6}$, i.e. $V_{\text{at}}/V_{\text{eff}} \approx 2^{1/2}$, where V_{eff} is the volume of the effective hard sphere. Thus, vitrification of molecular liquids under isothermal compression should occur when the density increases by 40%, which agrees well with the experimental results of Herbst et al. [19] (Fig. 12). For the 5–8 potential, used for transition metals [120], we get $V_{\text{at}}/V_{\text{eff}} \approx 8/5$, i.e. vitrification

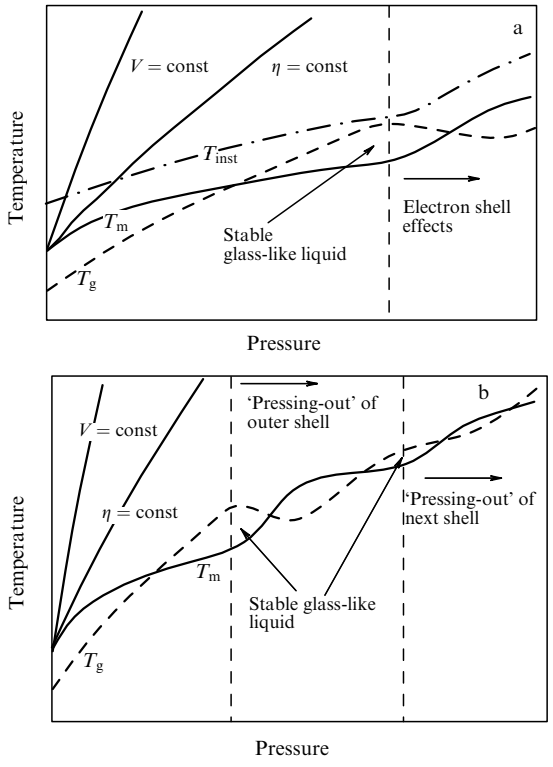

Figure 10. Hypothetical phase diagram of a metallic melt illustrating the relative position of the melting curve $T_m(P)$ and the vitrification line $T_g(P)$ and the possibility of their intersection. The figure also depicts the constant-volume lines $V = \text{const}$ and constant-viscosity lines $\eta = \text{const}$, and also the possible position of the mechanical instability line $T_{\text{inst}}(P)$ (spinodal) of the crystal phase (a). In view of the fact that the process of 'pressing-out' and delocalization of the core electrons must be of a successive and multistage nature due to the presence of several inner shells, hypothetically we can expect multiple intersections of the melting curve and the vitrification line (b).

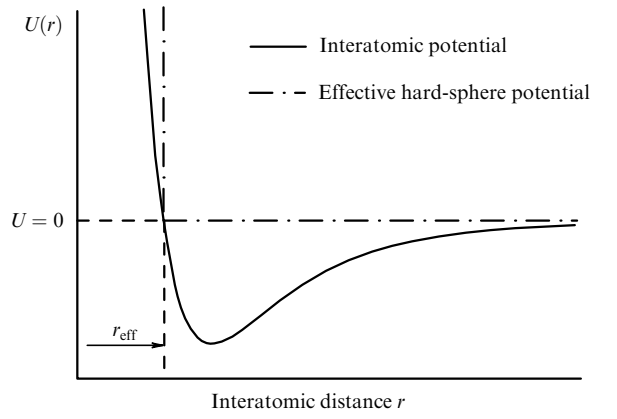

Figure 11. Replacement of a typical interatomic potential $U(r)$ with the potential of an infinitely hard sphere with infinitely weak attraction ($U \equiv 0$ for $r > r_{\text{eff}}$).

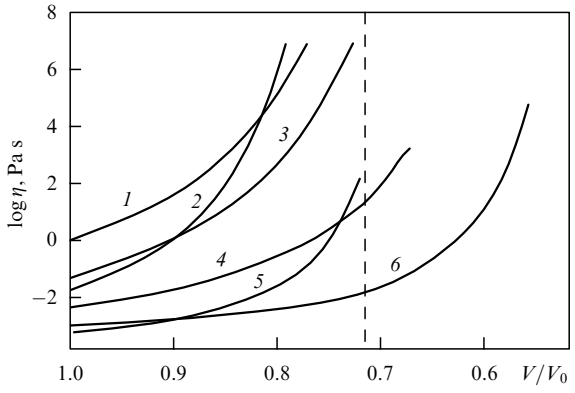

Figure 12. Comparison of the experimental curves representing the dependence of the viscosity of some organic liquids on the relative volume (the data was taken from Ref. [17]), and an estimate of the vitrification threshold for molecular liquids with a van der Waals interaction. The experimental curves correspond to the following substances, *1*, glycerin; *2*, dibutyl phthalate; *3*, 1,2-propanediol; *4*, 1-pentanol; *5*, toluene; and *6*, methanol.

of metals under isothermal compression should occur when the density increases by approximately 60%. The radius of the effective hard sphere decreases as the temperature grows. Estimates for iron made in accordance with the expressions in Ref. [125] yield

$$\frac{V_{\rm at}}{V_{\rm eff}} \sim 2-2.5 \qquad (32)$$

for $T \sim 5000$ K and $P \sim 3.3$ Mbar. We see that in the model of effective hard spheres, too, the glassy viscous state is attained when the density of the melt increases along the melting curve by a factor of approximately two.

The fact that the curves $T_{\rm g}(P)$ and $T_{\rm m}(P)$ intersect means that vitrification under compression is possible not only in the supercooled region (which is usually the case for organic liquids in the 20 – 80 kbar pressure range) but also in the P, T region of melt stability. Thus, when $T > T_{\rm m}$, an increase in the melt's viscosity may lead to a new state of the liquid with a viscosity value typical of glass. Note that earlier an assumption was repeatedly introduced according to which for some organic substances the relationship $T_{\rm g} > T_{\rm m}$ is met even at atmospheric pressure [83, 123], i.e. stable organic glasses were supposed to exist under normal pressure. This assumption was never verified by experiments, however. On the other hand, the transition of metallic melts under pressure into thermodynamically equilibrium metallic glasses is probably a universal phenomenon. Compression ratios for melts ranging from two to three along the melting curve correspond, for different metals, to a pressure in the 1 – 7 Mbar range, with the range of the respective melting points being 2000 – 8000 K. Many insulators and semiconductors become metals below 1 Mbar, with all the above reasoning remaining valid. Note that the 'pressing-out' of the electrons from the inner shells and the quantum phenomena that accompany compression usually manifest themselves from $P \sim 50$ Mbar, so that the use of the 'classical' approach to metallic melts in the 1 – 10 Mbar range is perfectly justified.

At pressures above the value at which the curves $T_{\rm g}(P)$ and $T_{\rm m}(P)$ intersect, the crystal 'melts' into a glassy state. The transition of the crystal into a liquid on heating takes place because of the increase in entropy at the transition. The entropy of the liquid is higher because of the possibility of realizing different atomic configurations in phase space [93]. At a viscosity typical of a glass ($> 10^{14}$ Pa s), the realization of a large number of configurations in the melt is achieved only during long or very long periods of time ($> 10^3$ s). This actually means long times for melting the crystal and the possibility of overheating it. Only pulse heating makes it possible to overheat (with respect to the equilibrium melting point) crystals whose melts have low viscosity. At the same time, for highly viscous melts a substantial overheating of the respective crystals is easily achieved [60]. For values of the viscosity of the melt characteristic of glass, the crystal will remain overheated, up to the vitrification point, in the course of ordinary experimental times. Thus, starting from certain pressures [near the point at which the curves $T_{\rm g}(P)$ and $T_{\rm m}(P)$ intersect], the experimentally measured melting point of a crystal differs from the thermodynamic quantity $T_{\rm m}$ and practically coincides with the vitrification point $T_{\rm g}$ of the melt. Without the use of special catalysts, reverse crystallization by cooling from a liquid state with a viscosity higher than $> 10^{14}$ Pa s is practically impossible. At temperatures $T > T_{\rm m}$ the stable glassy state is quite ergodic over long time intervals (similar to the case of a simple viscous liquid) and non-ergodic over short time intervals ($< 10^3$ s). In this way a highly viscous liquid differs from a metastable glassy state at temperatures $T < T_{\rm m}$, which is non-ergodic in principle, since over long time intervals such a state crystallizes and most realizations in phase space are absolutely unattainable.

For melts with low viscosities, the overheating on pulse heating is limited by the temperature at which the crystal lattice loses stability (the spinodal for the crystal) [60, 126]. Under ultra-high pressure the spinodal of the crystal probably always lies above the vitrification line $T_{\rm g}(P)$ (Fig. 10a).

As noted in Section 6, the viscosity of an electron – ion plasma with point nuclei (ions), i.e. without the electrons of the core, near the melting curve is not very high, and the corresponding vitrification point is probably below the melting point [95, 99]. Shell effects should be observed in metals in the 50 – 1000 Mbar range, namely, the 'pressing-out' of electrons from the inner shells to the band. Here one may observe a sharp rise in the melting point, since for an electron – ion plasma $T_{\rm m} \sim Z^2 \rho^{1/3}$, where Z is the ion charge. On the other hand, the vitrification point is determined primarily by the size and rigidity of the core and may become lower. As a result, in the 10 – 1000 Mbar range there may be multiple intersections of the curves $T_{\rm g}(P)$ and $T_{\rm m}(P)$ (Fig. 10b).

The behavior of the curves $T_{\rm g}(P)$ and $T_{\rm m}(P)$ during the transition of metals into the state of degenerate electron–ion plasma in the $10 – 10^4$ Mbar pressure range may be very complicated and merits a separate discussion, which lies outside the scope of the present review.

9. Conclusions

The conclusion that the viscosity of metal melts may grow by many orders of magnitude under compression is very important for the physics of the Earth and other planets. The results obtained in the present review may lead to an overhaul of many astrophysical concepts related to convection inside planets, magnetic fields and tidal forces of celestial bodies, the movements of the satellites of planets, and the

nutation of celestial bodies. We believe that the unexpected conclusion concerning the existence of a state of stable metallic glass (a 'thickened' liquid) in the megabar pressure range at temperatures above the melting point will be of special interest. The presence of a P, T region of stability of the melt with a viscosity characteristic of glass is to a great extent a challenge to the modern ideas about the nature of glass. We hope that the experimental studies of melts under megabar pressures and the theoretical calculations of atomic transport coefficients that use realistic interatomic potentials will help clarify the behavior of viscosity and diffusion in highly compressed melts of different types.

In conclusion we would like to express our gratitude to S M Stishov, V N Ryzhov, and S V Popova for the fruitful discussions. The work was supported financially by the Russian Fund for Basic Research (Grant 98-02-16325) and the Education and Scientific Center 'Matter in Conditions of High Static Compression' (Project No. 250).

References

1. Fortov V E *Usp. Fiz. Nauk* **138** 361 (1982) [*Sov. Phys. Usp.* **25** 781 (1982)]
2. Young D A *Phase Diagrams of the Elements* (Berkeley: Univ. of California Press, 1991)
3. Gryaznov V K et al. *Zh. Eksp. Teor. Fiz.* **114** 1242 (1998) [*JETP* **87** 678 (1998)]
4. Kirzhnits D A *Usp. Fiz. Nauk* **104** (3) 489 (1971) [*Sov. Phys. Usp.* **14** 512 (1972)]
5. Zharkov V N, Kalinin V A *Uravneniya Sostoyaniya Tverdykh Tel pri Vysokikh Davleniyakh i Temperaturakh* (Equations of State for Solids at High Pressures and Temperatures) (Moscow: Nauka, 1989) [English translation of a previous edition: (New York: Consultants Bureau, 1971)]
6. Zharkov V N, Trubitsyn V P *Physics of Planetary Interiors* (Tucson, Ariz.: Pachart Pub. House, 1978)
7. Anderson D L *Theory of the Earth* (Boston: Blackwell Sci. Publ., 1989)
8. Boehler R *Nature* (London) **363** 534 (1993)
9. Anderson 0 L *J. Geomag. Geoelectr.* **45** 1235 (1993)
10. Anderson W W, Ahrens T J *J. Geophys. Res.* **99** 4273 (1994)
11. Hubbard W *Planetary Interiors* (New York: Van Nostrand, 1984)
12. Bridgman P W *Collected Experimental Papers* Vol. VI (Cambridge, Mass.: Harvard Univ. Press, 1964) p. 2043
13. Bridgman P W *Collected Experimental Papers* Vol. VI (Cambridge, Mass.: Harvard Univ. Press, 1964) p. 3903
14. Slusar' V P, Rudenko N S, Tret'yakov V M, in *Teplofizicheskie Svoĭstva Veshchestv i Materialov* (Thermophysical Properties of Substances and Materials) Vol. 7 (Moscow: Izd-vo Standarty, 1973) p. 50
15. Munro R G, Piermarini G J, Block S *Rev. Phys. Chem. Jpn.* **50** 79 (1980)
16. Trappeniers N J, Van der Gulik P S, Van den Hooff H *Chem. Phys. Lett.* **70** 438 (1980)
17. Barnett J D, Bosco C D *J. Appl. Phys.* **40** 3144 (1969)
18. Sidorov V A, Tsiok O B *Fiz. Tekh. Vys. Davl.* **1** (3) 74 (1991)
19. Herbst C A, Cook R L, King H E (Jr.) *J. Non-Cryst. Solids* **172–174** 265 (1994)
20. Hsieh M, Swalin R A *Acta Metallurg.* **22** 219 (1974)
21. Spaepen F, in *Physics of Defects* (USMG/NATO ASI. Les Houches, Session XXXV, 1980, Eds R Balian, M Kl'eman, J-P Poirier) (Amsterdam: North-Holland, 1981) p. 133
22. Chaudhari P, Spaepen F, Steinhardt P, in *Glassy Metals II* (Eds H Beck, H-J Güntherodt) (Berlin: Springer, 1983)
23. Poirier J P *Geophys. J.* **92** 99 (1988)
24. Angelani L, Parisi G, Ruocco G, Viliani G *Phys. Rev. Lett.* **81** 4648 (1998)
25. Meyer A, Wuttke J, Petry W, Randl O G, Schober H *Phys. Rev. Lett.* **80** 4454 (1998)
26. Yamamoto R, Onuki A *Phys. Rev. Lett.* **81** 4915 (1998)
27. Perera D N, Harrowell P *Phys. Rev. Lett.* **81** 120 (1998)
28. Bridgman P W *Collected Experimental Papers* Vol. VI (Cambridge, Mass.: Harvard Univ. Press, 1964) p. 2155
29. Ozelton M W, Swalin R A *Philos. Mag.* **153** 441 (1968)
30. LeBlanc G E, Secco R A *Geophys. Res. Lett.* **23** 213 (1996)
31. Brazhkin V V et al. *Phys. Scripta* **39** 338 (1989)
32. Brazhkin V V, Popova S V, Voloshin R N *High Press. Res.* **6** 325 (1992)
33. Brazhkin V V et al. *High Press. Res.* **6** 333 (1992)
34. Brazhkin V V, Popova S V *Rasplavy* (4) 97 (1989)
35. Brazhkin V V, Popova S V *Rasplavy* (1) 10 (1990)
36. Brazhkin V V *Pis'ma Zh. Eksp. Teor. Fiz.* **68** 469 (1998) [*JETP Lett.* **68** 502 (1998)]
37. Keyes E W, in *Solids under Pressure* (Eds W Paul, D M Warschauer) (New York: McGraw-Hill, 1963) p. 71
38. Angell C A *Science* **267** 1924 (1995)
39. Kushiro I *J. Geophys. Res.* **81** 6347 (1976)
40. Sharma S K, Virgo D, Kushiro I *J. Non-Cryst. Solids* **33** 235 (1979)
41. Kushiro I, in *Physics of Magmatic Processes* (Ed. R B Hargraves) (Princeton, N.J.: Princeton Univ. Press, 1980) p. 93
42. Shimizu N, Kushiro I *Geochim. Cosmochim. Acta* **48** 1295 (1984)
43. Doi T *Rev. Phys. Chem. Jpn.* **33** 41 (1963)
44. Mineev V N, Savinov E V *Zh. Eksp. Teor. Fiz.* **52** 629 (1967) [*Sov. Phys. JETP* **25** 411 (1967)]
45. Mineev V N, Zaĭdel' R M *Zh. Eksp. Teor. Fiz.* **54** 1633 (1968) [*Sov. Phys. JETP* **27** 874 (1968)]
46. Mineev V N, Savinov E V *Zh. Eksp. Teor. Fiz.* **6**8 1321 (1975) [*Sov. Phys. JETP* **41** 656 (1975)]
47. Al'tshuler L V, Kanel' G I, Chekin B S *Zh. Eksp. Teor. Fiz.* **72** 663 (1977) [*Sov. Phys. JETP* **45** 348 (1977)]
48. Hamman S D, Linton M *J. Appl. Phys.* **40** 913 (1969)
49. *Svoĭstva Elementov: Spravochnik* (Properties of Elements: A Handbook) (Ed. M E Drits) (Moscow: Metallurgiya, 1985)
50. Kaye G W C, Laby T H *Tables of Physical and Chemical Constants* 9th ed. (New York: Longmans, 1943)
51. Shinyaev A Ya *Fazovye Prevrashcheniya i Svoĭstva Splavov pri Vysokom Davlenii* (Phase Transformations and Properties of Alloys under High Pressure) (Moscow: Nauka, 1973)
52. Lazarus D, Nachtrieb N H, in *Solids under Pressure* (Eds W Paul, D M Warschauer) (New York: McGraw-Hill, 1963) p. 43
53. Longuet-Higgins H C, Pople J A *J. Chem. Phys.* **25** 884 (1956)
54. Alder B J, Gass D M, Wainwright T E *J. Chem. Phys.* **53** 3813 (1970)
55. Chandler D *J. Chem. Phys.* **62** 1358 (1975)
56. Zhakhovskiĭ V V *Zh. Eksp. Teor. Fiz.* **105** 1615 (1994) [*JETP* **78** 871 (1994)]
57. Wallace D C *Phys. Rev. E* **58** 538 (1998)
58. Tonkov E Yu *High Pressure Phase Transformations: A Handbook* (Philadelphia: Gordon and Breach, 1992)
59. Rice S A, Nachtrieb N H *J. Chem. Phys.* **31** 139 (1959)
60. Ubbelohde A R *The Molten State of Matter* (New York: Wiley, 1978)
61. Andrade E N *Proc. R. Soc. London. Ser. A* **215** 36 (1952)
62. Souders M *J. Am. Chem. Soc.* **60** 154 (1938)
63. Sanditov D S, Bartenev G M *Fizicheskie Svoĭstva Neuporyadochennykh Struktur: Molekulyarno-Kineticheskie i Termodinamicheskie Protsessy v Neorganicheskikh Steklakh i Polimerakh* (Physical Properties of Disordered Structures: Molecular-Kinetic and Thermodynamic Processes in Inorganic Glasses and Polymers) (Novosibirsk: Nauka, 1982)
64. Doolittle A K *J. Appl. Phys.* **22** 1471 (1951)
65. Cohen M H, Turnbull D *J. Chem. Phys.* **31** 1164 (1959)
66. Woodcock L V, Angell C A *Phys. Rev. Lett.* **47** 1129 (1981)
67. Skripov V P, Faizullin M Z *High Temp. High Press.* **18** 1 (1986)
68. Fearn D R, Loper D E, Roberts P H *Nature* (London) **292** 232 (1981)
69. Kuznetsov V V *Usp. Fiz. Nauk* **167** 1001 (1997) [*Phys. Usp.* **40** 951 (1997)]
70. Song X, Richards P G *Nature* (London) **382** 221 (1996)
71. Whaler K, Hoime R *Nature* (London) **382** 205 (1996)
72. Su W-J, Dziewonski A M, Jeanioz R *Science* **274** 1883 (1996)
73. Song X D, Helmberger D V *Science* **282** 924 (1998)
74. Toomre A *Geophys. J. R. Astron. Soc.* **38** 335 (1974)
75. Anderson D L *Nature* (London) **285** 204 (1980)
76. Officer C B *J. Geophys.* **59** 89 (1986)

77. Vocadlo L et al. *Faraday Discuss.* **106** 205 (1997)
78. De Wijs G A et al. *Nature* (London) **392** 805 (1998)
79. Alfe D, Gillan M *Phys. Rev. B* **58** 8248 (1998)
80. Alfe D, Gillan M *Phys. Rev. Lett.* **81** 5161 (1998)
81. Ladbury R *Phys. Today* **49** (11) 21 (1996)
82. Glatzmaier G A, Roberts P H *Nature* (London) **377** 203 (1995)
83. Brazhkin V V "Vliyanie Vysokogo Davleniya na Zatverdevanie Metallicheskikh Rasplavov" (Pb, In, Cu, Dvoinye Splavy na Osnove Medi) (Effect of High Pressure on the Solidification of Metallic Melts (Pb, In, Cu, and Copper-Based Binary Alloys)), Ph.D. Thesis in Physics and Mathematics (Moscow, 1987)
84. Khvostantsev L G, Vereshchagin L F, Novikov A P *High Temp. High Press.* **9** 637 (1977)
85. Beck H, Güntherodt H-J, in *Glassy Metals I* (Eds H-J Güntherodt, H Beck) (Berlin: Springer, 1981)
86. *Metals Reference Book* 5th ed. (Ed. C J Smithells) (London: Butterworths, 1976)
87. Damask A C, Dienes G J *Point Defects in Metals* (New York: Gordon and Breach, 1971)
88. Kittel Ch *Introduction to Solid State Physics* 5th ed. (New York: Wiley, 1976) Ch. 20
89. Ruocco G et al. *Nature* (London) **379** 521 (1996)
90. Guinan M W, Steinberg D J *J. Phys. Chem. Solids* **35** 1501 (1974)
91. Hardy W H, Crawford R K, Daniels W B *J. Chem. Phys.* **54** 1005 (1971)
92. Crawford R K, in *Rare Gas Solids* Vol. II (Eds M L Klein, J A Venables) (London: Academic Press, 1977) Ch. 11
93. Stishov S M *Usp. Fiz. Nauk* **114** 3 (1974) [*Sov. Phys. Usp.* **17** 625 (1975)]
94. Hoover W G, Gray S G, Johnson K W *J. Chem. Phys.* **55** 1128 (1971)
95. Stevenson D J, Salpeter E E *Astrophys. J. Suppl. Ser.* **35** 221 (1977)
96. Ashcroft N W, Mermin N D *Solid State Physics* (New York: Holt, Rinehart and Winston, 1976)
97. Boehler R et al. *Rev. High Pressure Sci. Technol.* **1** 86 (1998)
98. Hansen J P, McDonald I R, Pollock E L *Phys. Rev. A* **11** 1025 (1975)
99. Vieillefosse P, Hansen J P *Phys. Rev. A* **12** 1106 (1975)
100. Smyle D E *Science* **284** 461 (1999)
101. Kerr R A *Science* **283** 1826 (1999)
102. Gutenberg B *Trans. Am. Geophys. Un.* **38** 750 (1957)
103. Söderlind P, Moriartry A, Wills J M *Phys. Rev. B* **53** 14063 (1996)
104. Steinle-Neumann G, Stixrude L, Cohen R E *Phys. Rev. B* **60** 791 (1999)
105. Singh A K, Mao Ho-Kwang, Shu J, Hemley R J *Phys. Rev. Lett.* **80** 2157 (1998)
106. Mao H-K. et al. *Nature* (London) **396** 741 (1998)
107. Kunze H-J, in *Glassy Metals II* (Eds H Beck, H-J Güntherodt) (Berlin: Springer, 1983)
108. Weaire D et al. *Acta Metallurg.* **19** 779 (1971)
109. Golding B, Bagley B G, Hsu F S L *Phys. Rev. Lett.* **29** 68 (1972)
110. Boehier R, Von Bargen N, Chopelas A *J. Geophys. Res.* **95** 21731 (1990)
111. Yoo C S, Holmes N C, Ross M, Webb D J, Pike C *Phys. Rev. Lett.* **70** 3931 (1993)
112. Williams Q et al. *Science* **236** 181 (1987)
113. Denisov G G, Novikov V V *Dokl. Ross. Akad. Nauk* **362** 484 (1998) [*Dokl. Phys.* **43** 630 (1998)]
114. Sidorenko V S *Astron. Vestnik* **27** 119 (1993)
115. Hide R, Dickey J O *Science* **253** 629 (1991)
116. Hoover W G et al. *J. Chem. Phys.* **52** 4931 (1970)
117. Bengtzelius U *Phys. Rev. A* **33** 3433 (1986)
118. Tölle A et al. *Phys. Rev. Lett.* **80** 2374 (1998)
119. Nauroth M, Kob W *Phys. Rev. E* **55** 657 (1997)
120. Wills J M, Harrison W A *Phys. Rev. B* **28** 4363 (1983)
121. Mishin Y, Farkas D, Mehl M J, Papaconstantopoulos D A *Phys. Rev. B* **59** 3393 (1999)
122. Hausleitner C, Hafner J *J. Phys. F* **18** 1025 (1988)
123. Feltz A *Amorphe und glasartige anorganische Festkörper* (Berlin: Akademie-Verlag, 1983) [Translated into English: *Amorphous Inorganic Materials and Glasses* (Weinheim: VCH, 1993)]
124. Shumway S L, Clarke A S, J'onsson H *J. Chem. Phys.* **102** 1796 (1995)
125. Ben-Amotz D, Herschbach D R *J. Phys. Chem.* **94** 1038 (1990)
126. Brazhkin V V, Lyapin A G *High Press. Res.* **15** 9 (1996)